Potential contributions of nitrifiers and denitrifiers to nitrous oxide sources and sinks in China's estuarine and coastal areas

Xiaofeng Dai[1], Mingming Chen[1], Xianhui Wan[2], Ehui Tan[3], Jialing Zeng[1], Nengwang Chen[1, 4], Shuh-Ji Kao[1, 3], Yao Zhang[1*]

[1]State Key Laboratory of Marine Environmental Science, College of Ocean and Earth Sciences, Xiamen University, Xiamen 361005, China

[2]Department of Geosciences, Princeton University, NJ 08540, USA.

[3]State Key Laboratory of Marine Resource Utilization in South China Sea, Hainan University, Haikou, Hainan, China

[4]Fujian Provincial Key Laboratory for Coastal Ecology and Environmental Studies, College of the Environment and Ecology, Xiamen University, Xiamen 361005, China

Correspondence to: Yao Zhang (yaozhang@xmu.edu.cn)

Abstract. Nitrous oxide (N_2O) is an important ozone-depleting greenhouse gas produced and consumed by microbially mediated nitrification and denitrification pathways. Estuaries are intensive N_2O emission regions in marine ecosystems. However, the potential contributions of nitrifiers and denitrifiers to N_2O sources and sinks in China's estuarine and coastal areas are poorly understood. The abundance and transcription of six key microbial functional genes involved in nitrification and denitrification, as well as the clade II-type *nosZ* gene-bearing community composition of N_2O reducers, were investigated in four estuaries spanning the Chinese coastline. The results showed that the ammonia-oxidizing archaeal *amoA* genes and transcripts were more dominant in the northern Bohai Sea (BS) and Yangtze River estuaries, which had low nitrogen concentrations, while the denitrifier *nirS* genes and transcripts were more dominant in the southern Jiulong River (JRE) and Pearl River estuaries, which had high levels of terrestrial nitrogen input. Notably, the *nosZ* clade II gene was more abundant than the clade I-type throughout the estuaries except for in the JRE and a few sites of the BS, while the opposite transcript distribution pattern was observed in these two estuaries. The gene and transcript distributions were significantly constrained by nitrogen and oxygen concentrations, as well as salinity, temperature, and pH. The *nosZ* clade II gene-bearing community composition along China's coastline had a high diversity and was distinctly different from that in the soil and marine oxygen-minimum-zone waters. By comparing

the gene distribution patterns across the estuaries with the distribution patterns of the N_2O concentration

and flux, we found that denitrification may principally control the N_2O emissions pattern.

1 Introduction

Nitrous oxide (N_2O) is a kind of ozone-depleting substance and an important, long-lived greenhouse gas

with 298 times the single mole global warming potential of carbon dioxide (CO_2) (IPCC 2007;

Ravishankara et al., 2009; Rowley et al., 2013). Prokaryotic microorganisms play an important role in

N_2O production and consumption through nitrification and denitrification pathways (Silvennoinen et al.,

2008; Santoro et al., 2011; Babbin et al., 2015; Domeignoz-Horta1 et al., 2015; Ji et al., 2018b; Meinhardt

et al., 2018). N_2O is produced as a byproduct in the first step ($NH_4^+ \rightarrow NO_2^-$) of nitrification, which is

catalyzed by ammonia monooxygenase in ammonia-oxidizing archaea (AOA) and ammonia-oxidizing

bacteria (AOB) (Codispoti and Christensen, 1985). The ammonia monooxygenase subunit A gene (*amoA*)

is frequently used as a functional gene marker for AOA and AOB analysis. N_2O is also produced as a

kind of intermediate product in the denitrification process, in which nitrite (NO_2^-) is reduced to nitric

oxide (NO) and then further reduced to N_2O. Usually, the nitrite reductase genes *nirS* and *nirK* are used

to evaluate the N_2O production potential through denitrification (Wrage et al., 2001; Shaw et al., 2006;

Hallin et al., 2018). Some bacterial nitrifiers can also reduce NO_2^- to N_2O through a nitrifier

denitrification pathway. The last step of denitrification is the only known biological N_2O consumption

pathway, reducing N_2O into nitrogen (N_2) under the catalysis of nitrous oxide reductase encoded by the

nosZ gene. This gene is divided into two clades according to the differences in the signal peptides of

nitrous oxide reductase (Henry et al., 2006; Jones et al., 2013). Intergenomic comparisons have revealed

that approximately 51% of the microorganisms possessing clade II-type *nosZ* genes lack nitrite reductase,

do not produce N_2O, and thus are expected to drive potential N_2O sinks (Jones et al., 2008; Sanford et

al., 2012; Marchant et al., 2017). The community composition of microorganisms with *nosZ* clade II

genes is considered important for the N_2O:N_2 end-product ratio of denitrification, influencing the

regional N_2O source or sink characteristics (Philippot, 2013; Domeignoz-Horta1 et al., 2015). However,

there are few studies on *nosZ* clade II gene diversity and community composition in Chinese estuarine

and coastal areas.

Biogeosciences
Discussions

60   Decades of research have revealed that the ocean is the second most important source of N_2O

emissions following arable soils, contributing one-third of the N_2O emission fluxes to the atmosphere

(Nevison et al., 2003). Estuaries, as important bioreactors, are the most active N_2O exchange areas in the

ocean, accounting for 33% of oceanic N_2O emissions with only approximately 0.4% of the area (Bange

et al., 1996; Zhang et al., 2010). Denitrification was the major contributor to N_2O production in terrestrial

65   ecosystems and stream and river networks (Beaulieu et al., 2011; Marzadri et al., 2017). However,

complete denitrification can consume N_2O (Jones et al., 2014). A recent study reported a fourfold

increase in global riverine N_2O emissions that was influenced by human activities (Yao et al., 2020).

Marine nitrification supported by ammonia-oxidizing archaea was largely responsible for oceanic N_2O

emissions, especially in the open ocean (Santoro et al., 2011; Löscher et al., 2012), while nitrate reduction

70   was the dominant N_2O source in oxygen minimum zones (OMZs) (Yamagishi et al., 2007; Ji et al.,

2018a). In estuaries, the transition zones between the land and sea, both nitrification and denitrification

could be dominant driving processes of active N_2O exchange. For example, nitrification was credited as

the dominant N_2O production pathway in the Schelde Estuary as well as in some other European estuaries

(De Wilde and De Bie, 2000; Barnes and Upstill-Goddard, 2011; Brase et al., 2017), while an inverse

75   correlation between N_2O concentration and oxygen indicated that sedimental denitrifiers might be the

dominant N_2O contributor in the Potomac River estuary (McElroy et al., 1978). In addition, research in

the Chesapeake Bay revealed that physical processes such as wind events and vertical mixing affected

the net balance between N_2O production and consumption, resulting in a variable source and sink for

N_2O (Laperriere et al., 2019).

80   The four main estuaries along the Chinese coastline include the Bohai Sea (BS) in the north, the

Yangtze River Estuary (YRE) and the adjacent East China Sea (ECS) in the middle, as well as the Jiulong

River Estuary (JRE) and Pearl River Estuary (PRE) in the south. The BS is a semi-enclosed sea located

in the north temperate zone of China. Influenced by frequent human activities and seasonal variability in

inputs from the Yellow River, Liao River, Luan River, and Hai River, seasonal hypoxia is an important

85   characteristic of the BS (Chen, 2009). The YRE and the adjacent ECS, which receive a large amount of

nutrients from the largest river in Asia (Yangtze River: runoff 9.2×10^{11} m^3 yr^{-1}) (Zhang, 2002), also

exhibited seasonal hypoxia off the estuary from July to September because of the enhanced primary

productivity (Zhu et al., 2011). Both the JRE and PRE are located in densely populated and industrialized

subtropical areas, with runoffs of 1.44×10^{10} m^3 yr^{-1} and 3.26×10^{11} m^3 yr^{-1}, respectively (Cao et al., 2005;

90   He et al., 2014). To clarify the potential contributions of nitrification and denitrification to sources and

sinks of N_2O in China's estuarine and coastal aeras, the abundance and transcription activity of six key

microbial functional genes involved in nitrification and denitrification (AOA and AOB *amoA*, *nirS*, *nirK*,

nosZ clade I and II genes) were investigated in the four estuarine areas. In addition, the *nosZ* clade II

gene diversity and N_2O reducing community composition were analyzed based on clone libraries to

95   assess the local N_2O sink potential.

2 Materials and methods

2.1 Sampling and biogeochemical parameter measurements

A total of 228 (130 for DNA and 98 for RNA) samples from fifty-four sites were collected (Fig. 1). One

100   hundred and sixteen samples (58 for DNA and for 58 for RNA) were collected from 20 stations with two

or three depth layers in the BS on the R/V Dongfanghong #2 from August to September 2018. Seventy-

four (41 for DNA and 33 for RNA) samples were collected from 16 stations with one to four depth layers

in the YRE on the R/V Yanping II from July to August 2017. Water samples were collected using a

rosette sampler fitted with Niskin bottles (SBE 911, Sea-Bird Co). Sixteen surface samples (9 for DNA

105   and 7 for RNA) from a water depth of ~0.5 m were collected from the JRE on the R/V Ocean II during

September 2016. Twenty-two samples for DNA were collected from 11 stations with two depth layers

in the PRE on the R/V Wanyu during January 2017. Water samples were collected using an organic glass

hydrophore (1 L; Kedun Co., China). In addition, 2 and 1 surface sediment samples were acquired using

a grab sampler from the JRE in December 2015 and from the YRE from July to August 2017, respectively.

110   Water samples of 0.2–2.5 L were filtered through 0.22 μm pore size polycarbonate membranes

(Millipore, USA) within 1 h at a <0.03 MPa pressure for quantitative PCR (qPCR) analysis. Water

samples were serially filtered through 10, 3, and 0.22 μm pore size polycarbonate membranes (Millipore,

USA) for clone library analysis (Table S1). The membranes for RNA extraction were immediately fixed

with 1.5 mL of RNAlater (Invitrogen, Life Technologies). All filters and sediment samples were quick-

115   frozen in liquid nitrogen and then stored at –80 °C for laboratory analysis.

Temperature, salinity, and depth were measured using conductivity temperature depth (CTD) (SBE 911, Sea-Bird Co.) in the BS, YRE, and PRE. In the JRE, water temperature and salinity were continuously measured (every 3 s for 1 min) using a YSI6600D salinometer installed on an underway pumping system (Yan et al., 2019). Dissolved oxygen (DO) concentrations were measured using a WTW

120 multiparameter portable meter (Multi 3430, Germany). Ammonia was analyzed on deck using the indophenol blue spectrophotometric method. Nitrate, nitrite, and silicate were measured using an AA3 Autoanalyzer (Bran+Luebbe Co., Germany) (Dai et al., 2008).

2.2 Nucleic acid extraction, clone library, and phylogenetic analysis

125 DNA from water samples was extracted using the phenol-chloroform-isoamyl alcohol method (Massana et al., 1997) with minor modifications. DNA from sediment samples was extracted using a FastDNA SPIN Kit for Soil (MP Biomedicals, USA). RNA from water samples was extracted using the RNeasy Mini kit according to the manual (Qiagen, USA). Clean RNA, which was verified by the amplification of the bacterial 16S rRNA gene with the primer set 342F/798R, was reverse transcribed to cDNA by the

130 SuperScript III first strand synthesis system (Invitrogen, Life Technologies) using random hexamers following the user manual. The quality of both the DNA and cDNA was checked by amplifying the full-length bacterial 16S rRNA gene before storage at –80 °C.

A total of 19 DNA samples (16 from water and 3 from sediment) from the four estuaries (Figs. 1 and 4) were used to construct clone libraries for the clade II-type *nosZ* gene. PCR was run with the primer

135 set nosZ-II-F (5'-CTIGGICCIYTKCAYAC-3') and nosZ-II-R (5'-GCIGARCARAAITCBGTRC-3') according to a previously reported reaction mixture and program (Jones et al., 2013) with the minor modification of using 10 µg of bovine serum albumin (BSA; Takara, Bio Inc.) instead of T4 gp32. PCR products were purified using an agarose gel DNA purification kit (Takara, Bio Inc.), ligated into the pMD19-T vector (Takara, Bio Inc.), and transformed into high-efficiency competent cells of *Escherichia*

140 *coli* according to the manufacturer's instructions. Forty to 127 positive *nosZ* clones were randomly selected from each library, reamplified using the vector primers M13-F and RV-M, and sequenced using ABI 3730 automated DNA sequence analyzer (Applied Biosystems). Poor-quality sequences with termination codons were manually checked and removed, and chimeras were removed using UCHIME (Edgar et al., 2011). All sequences were clustered into operational taxonomic units (OTUs) based on a

145   3% sequence divergence cutoff (Jones et al., 2014; Wittorf et al., 2020). Alpha diversity indices of the

clade II-type *nosZ* gene were calculated using the Usearch package (Edgar et al., 2010). The

representative sequences of OTUs were translated and analyzed with the BLASTp tool (*e*-value $<10^{-5}$).

The top 10 most similar sequences of each OTU were used as references. All sequences were aligned

using MAFFT (Katoh and Standley, 2013) and automatically trimmed using trimAl (Capella-Gutiérrez

150   et al., 2009). A maximum likelihood (ML) phylogenetic tree was constructed using Fasttree (v2.7.1,

default parameters) (Price et al., 2010) with 500 bootstrap replicates for node support determination.

2.3 Quantitative PCR of six functional genes

Archaeal *amoA,* bacterial *amoA*, *nirS*, *nirK*, *nosZ* clade I, and *nosZ* clade II genes were quantified by

155   qPCR with DNA and cDNA as templates using a CFX96 (Bio-Rad Laboratories, Singapore). Given the

relatively high ammonia concentration in the estuaries, the ammonia-oxidizing archaea (AOA) shallow

cluster (Water Column Cluster A; Francis et al., 2005) was targeted with the primer set Arch-amoAFA

and Arch-amoAR (Beman et al., 2008). Ammonia-oxidizing bacteria (AOB) are mostly affiliated with

two groups: Betaproteobacteria (*β*-AOB) and Gammaproteobacteria (*γ*-AOB) (Lam et al., 2007). Since

160   the latter was below detection limit in previous studies of Chinese estuaries (Zheng et al., 2017; Hou et

al., 2018), only *β*-AOB was targeted with the primer set amoA-1F and amoA-r New (Rotthauwe and

Witzel, 1997; Hornek et al., 2006). Bacterial *nirS* and *nirK* genes were quantified with the primer sets

nirS-1F and nirS-3R (Braker et al., 1998) and nirK876 and nirK1040 (Henry et al., 2004). Bacterial clade

I-type *nosZ* genes were quantified with the primer set nosZ2F and nosZ2R (Henry et al., 2006).

165   For the clade II-type *nosZ* gene quantification, the previously published primer sets were found to

have less than 80% amplification efficiency (Jones et al., 2013, 2014; Chee-Sanford et al., 2020). Here,

we designed a new primer set for use in our estuarine samples to quantify this gene. Representative

nucleotide sequences of each OTU obtained from the clone libraries derived from the PRE samples

(n=48) were translated into amino acid sequences and then aligned with the representative reference

170   sequences (n=116; covering 87 genera) obtained from the Functional Gene Repository

(http://fungene.cme.msu.edu/index.spr) by Clustal W. Two highly conserved regions containing five and

three amino acids in length were chosen to design new primer fragments. The new primer pairs and the

previously published nosZ-II-F and nosZ-II-R primer sets (Jones et al., 2013) were all evaluated by

175 Primer Premier 6.0, and eligible primer sets (GC content: 40–60%; optimal melting temperatures: 52–58 °C; stable 5' end and specific 3' end with no clamp or complementary structure) were tested by qPCR. The best primer combination was nosZ-II-F and the newly designed reverse primer (nosZ-II-Rnew: KGCRTAGTGIGGYTCDCC) with a ~325 bp target fragment length (Fig. S1). The qPCR system is shown in Table S2, and the optimized qPCR program was as follows: an initial 5 min denaturing step at 95 °C, followed by 35 cycles of 95 °C for 30 s, annealing at 53 °C for 60 s, 72 °C extension for 60 s and

180 a final extension at 72 °C for 10 min. The coverage of the primer sets was evaluated using the Search_pcr2 command of Usearch with the 116 reference sequences mentioned above and all clone sequences (n=1378) obtained from the clone libraries. A coverage of 93.5% (≤2 mismatches) was obtained for the new primer set.

The presence of PCR inhibitors in DNA extracts was examined by qPCR with different dilutions of

185 DNA (1-, 10-, and 100-fold dilutions). The samples with inhibitor were diluted 10 times to overcome the inhibitor effect according to our evaluation. Standard curves were constructed for the six genes using plasmid DNA from clone libraries generated from the PCR products. qPCRs were performed in triplicate and analyzed against a range of standards (10^1 to 10^8 copies per μL). All specific primer sequences and reactions for qPCR/PCR used in this study are shown in Table S2. The amplification efficiencies ranged

190 from 87% to 109% with R^2 >0.99 for each qPCR run. The specificity of qPCR products was verified by melting curves, agarose gel electrophoresis, and sequencing.

2.4 Statistical analysis

Redundancy analysis (RDA) based on qPCR or clone library data was used to analyze variations in the

195 gene/transcription distribution and *nosZ* clade II community composition under environmental constraints using R (R Core Team, 2017). The qPCR or clone library-based relative abundances and environmental factors were normalized via Z transformation (Magalhães et al., 2008). The collinearity between environmental parameters was excluded (variance inflation factors > 10; Palacin-Lizarbe et al., 2019). The null hypothesis that the community was independent of environmental parameters was tested

200 using constrained ordination with a Monte Carlo permutation test (999 permutations). Since a normal distribution of the individual datasets was not always met, we used the nonparametric Wilcoxon rank-sum tests for comparing two variables in GraphPad Prism software (San Diego, CA, USA). The bivariate

correlations were described by Spearman's (ρ value) or Pearson's (r value) correlation coefficients. False

discovery rate-based multiple comparison procedures were applied to evaluate the significance of

205 multiple hypotheses and identify truly significant comparisons (false discovery rate-adjusted *P* value)

(Pike, 2011).

3 Results
3.1 Environmental characteristics of the four estuaries

210 Water temperature increased with decreasing latitude from the BS (16.1–26.4 °C) to the YRE (19.2–

29.1 °C) and JRE (28.7–30.8 °C), where samples were all collected in summer. Samples were collected

in winter in the southernmost PRE, where the water temperature was 19.7–20.5 °C (Fig. 2). Salinity

exhibited consistently high values in all sites of the BS and YRE (26.4–34.6), except for two low values

(14.34 and 21.66) observed in the river mouth. In the JRE and PRE, obvious salinity gradients were

215 detected from 0.1 to 30.7. The DO concentration varied in the range of 4.25–8.46 mg L^{-1} in the BS, 1.25–

8.71 mg L^{-1} in the YRE, 4.04–6.89 mg L^{-1} in the JRE, and 2.22–9.22 mg L^{-1} in the PRE. There was a

distinct DO gradient from upstream to downstream of the PRE (Fig. 2). The dissolved inorganic nitrogen

(DIN: ammonium, nitrite, and nitrate) concentrations were generally lower in the BS and YRE compared

to those in the JRE and PRE. The ammonium concentration was in the range of 0.006–1.27 µM in the

220 BS, below detection (BD) to 1.99 µM in the YRE, 7.01–36.78 µM in the JRE, and 1.71–417.38 µM in

the PRE. The nitrite concentration was in the range of BD–5.65 µM in the BS and 0.004–2.5 µM in the

YRE, 7.24–30.87 µM in the JRE, and 0.41–69.23 µM in the PRE. The nitrate concentration ranged from

0.067–13.97 µM in the BS, 0.23–65.09 µM in the YRE, 24.94–241.32 µM in the JRE, and 3.0–320.53

µM in the PRE. Clear DIN concentration gradients were observed from upstream to downstream in the

225 JRE and PRE, particularly in the PRE.

3.2 Distribution of six key functional genes

The abundances of archaeal *amoA*, bacterial *amoA*, *nirS*, *nirK*, *nosZ* I, and *nosZ* II genes showed distinct

distribution patterns among the four estuaries (Figs. 3a–h). We divided the six genes into two groups for

230 analysis: one group included archaeal and bacterial *amoA*, *nirS*, and *nirK* genes indicating nitrification

and denitrification related to N$_2$O production (Figs. 3a–d), and the other included bacterial *nosZ* I and

nosZ II genes indicating N$_2$O consumption (Figs. 3e–h). In the gene group of N$_2$O production-related

processes, archaeal *amoA* was the most dominant in the BS (2.66×10^4–3.68×10^8 copies L^{-1}) and YRE

(4.86×10^3–9.47×10^7 copies L^{-1}) (Wilcoxon test, $P < 0.01$; Figs. 3a, b and Table S3), accounting for 3.96%

235   to 96.2% and 2.84% to 99.67%, respectively. In contrast to the northern estuaries, archaeal *amoA*

(5.28×10^5–4.40×10^6 copies L^{-1}) and bacterial *nirS* (2.57×10^5–6.29×10^6 copies L^{-1}) genes codominated

the gene group of N$_2$O production-related processes in the JRE (Fig. 3c), accounting for 2.43% to 72.93%

and 25.03% to 93.77%, respectively. In the southernmost PRE, the *nirS* gene was the most abundant

(3.48×10^4–1.66×10^9 copies L^{-1}), especially upstream ($P < 0.05$), accounting for 4.24% to 99.91% (Fig.

240   3d). Generally, archaeal *amoA* was widespread in all samples, and its abundance decreased from north

to south with differences of one to two magnitudes. A similar pattern was observed for bacterial *amoA*,

with lower abundances than archaeal *amoA* (Table S3). The abundance of the *nirS* gene was highest in

the PRE among the four estuaries, while the highest number of copies of the *nirK* gene was present in

the BS (Table S3). Among the different water depths, only the bacterial *amoA* and *nirS* genes in the BS

245   were observed to be more highly distributed in the middle and bottom layers than in the surface layer by

one to three orders of magnitude ($P < 0.05$).

In the N$_2$O-consuming genes, the abundances of the clade II-type *nosZ* gene were 6.55×10^3 to

2.24×10^7 copies L^{-1} in the BS (Fig. 3e), 6.14×10^3 to 8.11×10^6 copies L^{-1} in the YRE (Fig. 3f), and BD to

1.17×10^7 copies L^{-1} in the PRE (Fig. 3h), outnumbering the clade I-type ($P < 0.01$), with no significant

250   differences among the three estuaries. However, the clade II-type *nosZ* gene was below the detection

limit in the JRE, and only the clade I-type was detected with a range of 7.15×10^3–2.32×10^5 copies L^{-1}

(Fig. 3g and Table S3). The numbers of copies of the clade I-type *nosZ* gene were higher in the BS

estuary than in the other three estuaries ($P < 0.01$).

255   **3.3 Transcription activity of six key functional genes**

For the four genes of N$_2$O production-related processes, a generally similar relative abundance

distribution pattern was observed between transcripts and genes in the BS (Fig. 3i). Archaeal *amoA* gene

transcripts (3.51×10^3–1.62×10^6 transcripts L^{-1}) were significantly more abundant than other transcripts

($P < 0.01$), accounting for 37.94% to 99.30% of the total abundance of gene transcripts (Table S4).

260   Slightly different from the gene distribution in which the number of copies of the bacterial *amoA* gene

was relatively more abundant than that of the archaeal *amoA* gene in the river mouth of the YRE (Fig.

3b), the archaeal *amoA* gene transcript was abundant in the whole YRE, accounting for 9.1% to 100% of

the total abundance of gene transcripts, with a dominant abundance of *nirS* gene transcripts in a few

samples (Fig. 3j). A different distribution pattern was also observed between transcripts and genes in the

265   JRE (Figs. 3c, k). Bacterial *amoA* (7.06×10^5–8.22×10^7 transcripts L^{-1}) rather than archaeal *amoA*

transcripts ($P < 0.05$) were codominant with *nirS* transcripts (5.96×10^5–2.31×10^7 transcripts L^{-1}) (Fig.

3k). Notably, the total gene transcript abundance of N_2O production-related processes was higher in the

JRE (1.31×10^6–9.76×10^7 transcripts L^{-1}) than in the BS and YRE (3.03×10^2–1.12×10^6 transcripts L^{-1}) (*P*

< 0.01; Table S4). Bacterial *amoA* gene transcripts, consistent with the gene distribution, significantly

270   increased with depth in the BS ($P < 0.05$). No significant differences in transcript abundance were

observed among different depths for the six functional genes in the YRE.

For the N_2O-consuming genes, only the clade I-type *nosZ* gene transcript was determined (26.2–

2.34×10^3 transcripts L^{-1}), while the clade II-type *nosZ* gene transcript was below the detection limit in

the BS (Fig. 3l; Table S4). However, the *nosZ* II gene transcripts (bellow detection to 1.81×10^5 transcripts

275   L^{-1}) dominated most stations in the YRE, except for a dominant distribution of the *nosZ* I gene transcript

in the river mouth (Fig. 3m). Similar to the gene distribution, in the JRE, only the *nosZ* I gene transcript

was determined (1.23×10^3–5.37×10^4 transcripts L^{-1}) (Fig. 3n). No RNA samples were obtained in the

PRE.

280   **3.4 Phylogenetic diversity of the clade II *nosZ* gene**

Clone libraries of *nosZ* clade II were constructed for 19 samples from the four estuaries, resulting in a

total of 1378 quality-controlled sequences that were clustered into 441 OTUs at a similarity level of 97%.

The sequencing coverage for each clone library ranged from 73.9 to 96.2%. Higher gene diversity of

nosZ clade II was observed in the water and sediment samples from the JRE and the sediment sample

285   from the YRE than in the other samples (Fig. S2a). The rarefaction curves of the samples from JRE and

the sediment sample from YRE did not reach a plateau (data not shown), suggesting that some of the

diversity of *nosZ* clade II remained unsampled. Phylogenetic analysis of the representative sequences of

all the OTUs indicated that the clade II *nosZ* gene sequences were grouped with Bacteroidetes,

Proteobacteria, Actinobacteria, Chloroflexi, Chlorobi, Ignavibacteriae, Gemmatimonadetes,

290   Cyanobacteria, and Acidobacteria, in which the OTUs affiliated with Bacteroidetes, Proteobacteria,

Chloroflexi, and Actinobacteria were generally abundant among all samples (Fig. 4a). The OTUs belonging to Bacteroidetes were divided into two clusters according to the topological structure of the phylogenetic tree. One cluster contained the reference sequences mainly from marine habitats and the OTU sequences retrieved from the four estuaries, while the other cluster included the reference sequences

295   mainly from terrestrial habitats and the OTU sequences retrieved only from the low-latitude subtropical estuaries JRE and PRE. The OTU sequences affiliated with Alpha-, Gamma-, Delta-, Epsilonproteobacteria, and Actinobacteria were retrieved from the four estuaries, and the reference sequences were mainly from marine habitats, while the OTUs related to Betaproteobacteria, Oligoflexia, Chlorobi, and *Candidatus Melainabacteria* were retrieved only from the subtropical estuaries (JRE and

300   PRE), and the reference sequences were mainly from terrestrial habitats (Fig. 4a). Most known clusters of *nosZ* clade II can be found in our libraries, including a recently identified widespread clade II-type *nosZ* gene affiliated with the class Oligoflexia (Nakai et al., 2014).

A community structure shift of *nosZ* clade II was observed among the four estuaries (Fig. 4b). Bacteroidetes was the most dominant group in the samples from the BS (39.0–68.5%), followed by

305   Proteobacteria (Gamma-, Delta-, and Alphaproteobacteria; 18.7–26.0%). The sequences phylogenetically grouped into Proteobacteria (Gamma-, Delta-, and Epsilonproteobacteria; 23.0–70.6%) dominated the clone libraries from the YRE, followed by Chloroflexi (6.9–47.3%). The sequences from the JRE were also mainly affiliated with Proteobacteria (Beta-, Gamma-, Delta-, and Alphaproteobacteria and Oligoflexia; 11.8–40.5%), Bacteroidetes (30.9–37.9%), and Chloroflexi (12.1–50.9%). In contrast

310   to the three estuaries, the sequences affiliated with Bacteroidetes were absolutely dominant in the clone libraries of the PRE (>69.2%). A nonmetric multidimensional scaling (NMDS) analysis indicated that *nosZ* clade II communities from the same estuary were clustered together at a >10% similarity level, except for a separate cluster of the sediment community from the YRE (Fig. S2b). The *nosZ* clade II communities from the southern estuaries (JRE and PRE) and northern estuaries (YRE and BS) were

315   clustered separately at a >3% similarity level.

3.5 Correlations between six key functional genes and environmental factors

Variations in the gene/transcript distributions under environmental constraints were analyzed by RDA. The first two RDA axes explained 19.98% and 5.36% of the total variation in the gene – environment

320   relationship (Fig. 5a). Salinity, DO, nitrite, and ammonium concentrations were significantly correlated

with gene distribution ($P < 0.01$). The main variation in N_2O source or sink process-related genetic

potentials was across a *nirS* vs. archaeal *amoA* abundance gradient. The *nirS*-rich samples corresponded

to those from the southern estuaries (JRE and PRE) with higher ammonium and nitrite concentrations.

In contrast, the samples with the highest abundance of archaeal *amoA* were located in sites with high

325   salinity and low ammonium concentrations in the northern estuaries (BS and YRE). Notably, RDA of

the gene transcripts and environmental variables clearly separated the transcripts from different estuaries

along the axes, which explained 26.4% and 8.27% of the total variation (Fig. 5b). Variation in transcript

distribution was significantly correlated with pH, temperature, nitrite, and nitrate concentration ($P <$

0.01). The main variation of these transcripts was distributed across archaeal and bacterial *amoA* vs. *nosZ*

330   clade II abundance gradients. The archaeal *amoA* transcript-rich samples corresponded to those from the

BS and YRE sites with lower temperatures. The bacterial *amoA* gene was actively transcribed in the JRE

and positively correlated with nitrite and nitrate concentrations. The *nosZ* clade II transcript-rich samples

corresponded to those from the YRE sites with relatively higher pH and temperature. The *nosZ* clade I

and *nirS* transcript distributions were also positively correlated with pH and temperature, respectively.

335   RDA based on the clone library data of the clade II-type *nosZ* gene revealed that the *nosZ* II

community composition was significantly affected by temperature ($P < 0.01$; Fig. 5c). The first two RDA

axes explained 33.29% and 13.24% of the total variation. The *nosZ* II gene community compositions in

the BS may prefer environments with relatively high salinity and temperature. The community

compositions in the JRE water may prefer environments with a high temperature (the sediment samples

340   were not included in this analysis due to a lack of biogeochemical parameters). The *nosZ* clade II

microbes in the PRE and YRE may prefer to distribute in environments with high ammonium

concentrations.

4 Discussion

345   **4.1 Spatial niche differentiation of functional genes controlled by environmental factors**

There was a distinct large-scale spatial structure among the detected genes, as shown in Fig. 3.

Comparing the relative contributions of these functional genes to the total number of gene copies across

the study regions, there was a strong negative correlation between the relative abundances of the archaeal

amoA gene and bacterial *nirS* gene ($\rho = -0.89$, $P < 0.01$), and they showed contrasting patterns along

350 salinity and DIN gradients (Fig. S3). Samples from the BS and YRE exhibited high salinity and low DIN

concentrations. The high abundance of the archaeal *amoA* gene in these areas was consistent with

previous findings of nitrifiers comprised predominantly of AOA in estuarine environments with higher

salinity and lower ammonia concentrations because archaeal nitrifiers exhibit a high ammonia affinity

and salinity tolerance (Martens-Habbena et al., 2009; Abell et al., 2010; Bernhard et al., 2010; Zhang et

355 al., 2014; Hou et al., 2018; Hink et al., 2018; Ma et al., 2019). In contrast, both the JRE and PRE are

typical subtropical eutrophic estuaries with high DIN inputs from surrounding environments (Cao et al.,

2005; Yan et al., 2012b; He et al., 2014). Denitrifying bacteria are more adaptable to environments with

high organic carbon and nitrogen concentrations because they usually have high requirements for

substrates (Braker et al., 2000; Smith et al., 2007; Mosier and Francis, 2010; Wang et al., 2014; Wei et

360 al., 2015; Lee and Francis, 2017). The presence of nitrogen oxides was also shown to activate *nirK* and

nirS gene expression under anoxic conditions (Riya et al., 2017). Thus, the *nirS*-containing group was

more abundant upstream of the JRE and PRE. The significant correlations between DIN and the *nirS*

gene (Fig. S3) and transcript ($\rho = 0.341$, $P < 0.01$; data not shown) were consistent with a previous

conclusion that high anthropogenic N loading stimulates denitrification (Cole and Caraco, 2001; Garnier

365 et al., 2006; Beaulieu et al., 2011; Yan et al., 2012a).

Previous studies of N_2O-consuming gene abundance were mainly focused on terrigenous

ecosystems, e.g., in soil samples, the clade I- and II-type *nosZ* genes ranged from 10^4 to 10^8 and 10^4 to

10^7 copies g dry soil^{-1}, respectively (Jones et al., 2013, 2014). In marine ecosystems, only the oxygen-

depleted waters and coastal sediments were investigated, where the clade I-type was approximately 10^5

370 copies L^{-1} and both clades I and II ranged from 10^5–10^7 copies g wet sediment^{-1}, respectively (Wittorf et

al., 2020; Sun et al., 2021). We detected that the number of copies of the *nosZ* gene ranged from 6.59×10^3

to 2.35×10^8 copies L^{-1}, with an average of 4.94×10^6 copies L^{-1}, in China's estuarine and coastal areas.

There was a strong negative correlation between the relative abundance of the clade I- and II-type *nosZ*

genes ($\rho = -1$, $P < 0.01$), indicating that the two types were affiliated with different groups. The

375 distribution of *nosZ* (clades I and II) gene transcripts was significantly positively correlated with pH (Fig.

5b), suggesting that acidification of the ocean may accelerate N_2O emissions. N_2O production influenced

by pH has been observed in N-cycling water engineering systems and terrestrial ecosystems (Mørkved et al., 2007; Blum et al., 2018). Therefore, some studies have suggested that liming for acidic soils could mitigate N_2O emissions (McMillan et al., 2016; Wang et al., 2017; Senbayram et al., 2019). DO also

380   shows an important influence on denitrifying genes, which was consistent with a previous conclusion that O_2 concentration can impact the expression and metabolism of denitrification genes through protein sensing of oxygen conditions (Qu et al., 2016; Riya et al., 2017). Notably, we found that the distribution and abundance of the *nosZ* gene and the *nirS* or *nirK* genes were distinctly different, indicating that these functional genes were affiliated with different denitrifiers. This may be because not all N_2O-consuming

385   bacteria contain all denitrification genes (Sanford et al., 2012).

4.2 Gene transcription expression controlled by environmental factors

The gene transcript abundance showed a certain regional distribution difference with gene abundance (Fig. 3), suggesting that environmental factors might have different influences on gene distribution and

390   transcript activity. The bacterial *amoA* gene was transcribed actively in the JRE, although the archaeal *amoA* gene prevailed in gene abundance. Frequent water exchange may result in a large amount of the archaeal *amoA* gene from the ocean, but AOB were more active under high ammonium and low salinity conditions. AOB have been indicated to be the primary N_2O producer, even in an AOA-dominated environment (Meinhardt et al., 2018). Meta-analysis also revealed that AOB respond more strongly than

395   AOA to nitrogen addition (Carey et al., 2016). High abundances of bacterial *amoA* and *nirS* gene transcripts make the JRE a more potentially active area of N_2O production compared to the northern estuarine and coastal areas, which may be attributed to its high nitrogen input from surrounding environments. In contrast, in the mouth of the YRE, although the bacterial *amoA* gene contributed a large proportion of the gene abundance, the archaeal *amoA* gene was transcribed more actively. Flushing water

400   from the Yangtze River may transport a large amount of the bacterial *amoA* gene, but the archaeal *amoA* gene was more competitive in low ammonium and oxygen environments (Fig. 2) since the enzyme ammonia monooxygenase in AOA has a higher affinity for ammonia and a lower oxygen requirement than the AOB (Park et al., 2010; Martens-Habbena and Stahl, 2011).

405   **4.3 N_2O emissions potential implied by functional gene distribution**

The community structure of nitrifiers and denitrifiers was thought to have an important influence on N_2O emissions. For example, the abundance and expression of the archaeal *amoA* gene showed comparable patterns with N_2O production in the OMZ of the eastern tropical North Atlantic (Löscher et al., 2012). Inhibition of the abundance of bacterial *amoA* genes in hyperthermophilic composting was proven to

410 decrease N_2O emissions (Cui et al., 2019). The expression of the *nirK* gene induced by the addition of nitrate caused an increase in N_2O production in an anoxic soil slurry experiment (Riya et al., 2017). Transcription of clade I-type *nosZ* mRNA in the lower N_2O emission system was one order of magnitude higher than that in the higher N_2O emission system in wastewater treatment plants (Song et al., 2014). To assess how community structure controls the regional N_2O source or sink potential across China's

415 estuaries, we analyzed the relationships between N_2O concentration, N_2O flux, and ΔN_2O (data collected from the literature below) and the six functional gene distributions across the four estuaries. The N_2O concentration, N_2O flux, and ΔN_2O all showed an increasing distribution pattern from the northern, high-latitude to the southern, low-latitude estuaries (Figs. 6a–c), with hot spots in the north and center of the BS, nearshore of the YRE, and upstream of the JRE and PRE (Qinji, 2005; Chen et al., 2008; Zhang et

420 al., 2008; Wu et al., 2013; Song et al., 2015; Wang et al., 2016; Ma et al., 2019; Lin et al., 2020). Notably, total *amoA* gene abundances displayed a contrary pattern, while total *nir* gene abundances and the ratio of total *nir* to *amoA* gene abundances (*nir/amoA*) had generally consistent patterns with the N_2O concentration, N_2O flux, and ΔN_2O across the four estuaries (Figs. 6d–f). A significant correlation was even observed between the N_2O flux and the *nir/amoA* ratio based on the four averages of the four

425 estuaries (r = 0.95, n = 4, $P < 0.05$). Therefore, the *nir/amoA* ratio can indicate the N_2O emission potential in China's estuaries, which was consistent with previous findings that the N_2O production yield of denitrification was higher than that of nitrification in the lab and in situ experiments (Kester et al., 1997; Löscher et al., 2012; Stieglmeier et al., 2014; Frey et al., 2019).

Notably, the total *nosZ* gene abundance of N_2O-reducing denitrifiers seemed to have a contrasting

430 distribution pattern with the N_2O concentration, N_2O flux, and ΔN_2O across the four estuaries, with higher abundances in the high-latitude BS and lower abundances in the low-latitude JRE (Fig. 6g). The total *nosZ* gene abundances were one to two orders of magnitude lower than the total *nir* gene abundances in the JRE and PRE, where the N_2O concentration and flux were higher than those in the BS and YRE.

This indicated a distinctly higher denitrification-derived N_2O emission potential in the JRE and PRE.

435   The ratio of total *nir* to *nosZ* clade I gene abundances (*nir/nosZ* I) had a highly similar pattern with the N_2O concentration, N_2O flux, and ΔN_2O across the four estuaries in general (Fig. 6h), and significant correlations were also observed between the N_2O flux and *nir/nosZ* I (r = 0.97, n = 4, $P < 0.05$). Therefore, the *nir/nosZ* I ratio could be a better indicator of N_2O emission potential in China's estuaries. Abundances and activities of the N_2O-producing (*nirS* or *nirK*–bearing) community relative to the N_2O-reducing

440   (*nosZ*-bearing) community have also been used to assess the N_2O emission potential of soils (Thompson, 2016; Zhao et al., 2018). The high load of DIN in estuaries could be responsible for the high denitrification-derived N_2O emission potential. Both the *nir/nosZ* and *nir/amoA* ratios were positively correlated with the NH_4^+, NO_3^-, and NO_2^- concentrations (Spearman's $\rho = 0.32$–0.68, n = 114–122, $P < 0.01$ for each) and negatively correlated with salinity (Spearman's $\rho = -0.45$—0.66, n = 114–122, $P < $

445   0.01 for each). Previous studies in the YRE have proven that nitrogen input accelerates N_2O production in estuaries (Zhang et al., 2010; Yan et al., 2012a). Therefore, sufficient supplies of substrates may support high rates of denitrification and thus high N_2O emissions.

4.4 Influence of N_2O emissions by N_2O reducer composition

450   The community structure and diversity of the clade II *nosZ* gene retrieved from China's estuaries were different from those previously reported in soil and marine OMZ water (e.g., in the eastern tropical South and North Pacific and Arabian Sea) (Jones et al., 2013, 2014; Sun, 2020). The dominant *nosZ* clade II-bearing groups were affiliated with Bacteroidetes, Chloroflexi, Gamma-, and Betaproteobacteria in our four estuarine and coastal areas. However, the most abundant *nosZ* clade II groups found in the OMZ

455   were affiliated with *Anaeromyxobacter* (Deltaproteobacteria) and *Marinobacter* (Gammaproteobacteria) (Sun, 2020). The *nosZ* clade II organisms from terrestrial systems showed distinctly higher diversity (Sanford et al., 2012; Jones et al., 2014; Hallin et al., 2018; Zhao et al., 2018; Kato et al., 2018). The phylogenetically distinct predominant N_2O reducers can influence N_2O emissions directly or indirectly (Song et al., 2014). According to genomic information, *nosZ* clade II carriers affiliated with

460   Deltaproteobacteria and Chlorobi have neither the *nirK* nor *nirS* gene, and less than half of *nosZ* clade II organisms affiliated with Bacteroidetes, Chloroflexi, Gamma-, and Epsilonproteobacteria harbor the *nirK* or *nirS* gene, while all of the *nosZ* clade II microbes affiliated with Alpha- and Betaproteobacteria

also have the *nirS* gene (Hallin et al., 2018). Therefore, the distinct *nosZ* clade II community structure among the four estuaries may contribute to their different N_2O emissions potential. For example,

465 distinctly high diversity of the *nosZ* clade II gene was retrieved from the JRE water and sediment samples as well as the YRE sediment sample compared to the other estuaries. The high diversity of the *nosZ* clade II gene may be caused by the high temperature (e.g., in the low-latitude JRE) and sufficient nutrients at those sites. Previous studies have also indicated that the biodiversity of denitrifying bacteria increased in high-temperature seasons (Castellano-Hinojosa et al., 2017) and that nitrogen availability had a

470 positive effect on denitrifying bacteria in boreal lakes (Rissanen et al., 2011). In addition, the habitat type may also affect the abundance and diversity of N_2O-reducing communities, e.g., silty mud and sandy sediments had higher genetic potentials for N_2O reduction than cyanobacterial mat and *Ruppia maritima* meadow sediments (Wittorf et al., 2020).

475 **5 Summary**

This study revealed the distinct distribution patterns of six key microbial functional genes and transcripts related to N_2O production and consumption pathways in the BS, the YRE, the adjacent ECS, the JRE, and the PRE. The archaeal *amoA* genes and transcripts were more abundant in the northern BS, YRE, and the adjacent ECS, while the denitrifier *nirS* genes and transcripts were more abundant in the southern

480 JRE and PRE. The *nosZ* clade II gene was more abundant than the clade I-type throughout the estuaries except for in the JRE and a few sites of the BS, while the opposite transcript distribution pattern was observed in these two estuaries. Water mass parameters (temperature and salinity), substrates (ammonia/ammonium, nitrite, and nitrate), and influencing parameters of substrate availability (DO and pH) regulated the gene, transcript, and community composition distribution patterns. The community

485 structure of the clade II-type *nosZ* gene retrieved from China's estuaries was distinctly different from those of the soil and marine OMZ. Furthermore, combined with the N_2O concentration, flux, and ΔN_2O data collected from previous studies, our analysis found that although both the clade I- and II-type *nosZ* genes of N_2O reducers were widely distributed in these estuaries, N_2O production by the denitrification pathway may be more important in determining the N_2O emissions patterns across the estuaries. Nitrogen

490 loads may influence the N_2O source and sink processes by regulating the distribution of the related functional microbial groups.

Biogeosciences
Discussions

Open Access

EGU

Data availability

All quality-controlled sequences were submitted to GenBank with accession numbers OM567739–

495 OM568649. All other data can be accessed in the form of Excel spreadsheets via the corresponding

author.

Supplement

The Supplement related to this article is available online.

500

Author contributions

YZ conceived and designed the study. XD, XW, MC, ET, and NC performed the experiments and

auxiliary data collection. XD analyzed the data. XD and YZ wrote the paper. All authors contributed to

the interpretation of the results and critical revision.

505

Competing interests

The authors declare no conflicts of interest.

References

Abell, G. C. J., Revill, A. T., Smith, C., Bissett, A. P., Volkman, J. K., and Robert, S. S.: Archaeal

520 ammonia oxidizers and *nirS*-type denitrifiers dominate sediment nitrifying and denitrifying populations

in a subtropical macrotidal estuary, ISME J, 4(2), 286–300, doi:10.1038/ismej.2009.105, 2010.

Babbin, A. R., Bianchi, D., Jayakumar, A., and Ward, B. B.: Rapid nitrous oxide cycling in the suboxic

ocean, Science., 348(6239), 1127–1129, doi:10.1126/science.aaa8380, 2015.

Bange, H. W., Rapsomanik, S., and Andreae, M. O.: Nitrous oxide in coastal waters, Global Biogeochem.

525   Cycles, 10(1), 197–207, doi:10.1029/95GB03834, 1996.

Barnes, J. and Upstill-Goddard, R. C.: N_2O seasonal distributions and air-sea exchange in UK estuaries:

Implications for the tropospheric N_2O source from European coastal waters, J. Geophys. Res.

Biogeosciences, 116(1), doi:10.1029/2009JG001156, 2011.

Beaulieu, J. J., Tank, J. L., Hamilton, S. K., Wollheim, W. M., Hall, R. O., Mulholland, P. J., Peterson,

530   B. J., Ashkenas, L. R., Cooper, L. W., Dahm, C. N., Dodds, W. K., Grimm, N. B., Johnson, S. L.,

McDowell, W. H., Poole, G. C., Maurice Valett, H., Arango, C. P., Bernot, M. J., Burgin, A. J., Crenshaw,

C. L., Helton, A. M., Johnson, L. T., O'Brien, J. M., Potter, J. D., Sheibley, R. W., Sobota, D. J. and

Thomas, S. M.: Nitrous oxide emission from denitrification in stream and river networks, Proc. Natl.

Acad. Sci. U. S. A., 108(1), 214–219, doi:10.1073/pnas.1011464108, 2011.

535   Beman, J. M., Popp, B. N., and Francis, C.: Molecular and biogeochemical evidence for ammonia

oxidation by marine Crenarchaeota in the Gulf of California, ISME J. 2, 429–441,

doi:10.1038/ismej.2008.33, 2008.

Bernhard, A. E., Landry, Z. C., Blevins, A., De La Torre, J. R., Giblin, A. E. and Stahl, D. A.: Abundance

of ammonia-oxidizing archaea and bacteria along an estuarine salinity gradient in relation to potential

540   nitrification rates, Appl. Environ. Microbiol., 76(4), 1285–1289, doi:10.1128/AEM.02018-09, 2010.

Blum, J. M., Su, Q., Ma, Y., Valverde-Pérez, B., Domingo-Félez, C., Jensen, M. M. and Smets, B. F.:

The pH dependency of N-converting enzymatic processes, pathways and microbes: effect on net N_2O

production, Environ. Microbiol., 20(5), 1623–1640, doi:10.1111/1462-2920.14063, 2018.

Braker, G., Zhou, J., Wu, L., Devol, A. H. and Tiedje, J. M.: Nitrite reductase genes (*nirK* and *nirS*) as

545   functional markers to investigate diversity of denitrifying bacteria in Pacific northwest marine sediment

communities, Appl. Environ. Microbiol., 66(5), 2096–2104, doi:10.1128/AEM.66.5.2096-2104, 2000.

Brase, L., Bange, H. W., Lendt, R., Sanders, T. and Dähnke, K.: High resolution measurements of nitrous

oxide (N_2O) in the Elbe estuary, Front. Mar. Sci., 4, doi:10.3389/fmars.2017.00162, 2017.

Cao, W., Hong, H. and Yue, S.: Modelling agricultural nitrogen contributions to the Jiulong River estuary

550   and   coastal   water,   Glob.   Planet.   Change,   47(2-4   SPEC.   ISS.),   111–121,

doi:10.1016/j.gloplacha.2004.10.006, 2005.

Capella-Gutiérrez, S., Silla-Martínez, J. M. and Gabaldón, T.: trimAl: A tool for automated alignment trimming in large-scale phylogenetic analyses, Bioinformatics, 25(15), 1972–1973, doi:10.1093/bioinformatics/btp348, 2009.

555   Carey, C. J., Dove, N. C., Beman, J. M., Hart, S. C. and Aronson, E. L.: Meta-analysis reveals ammonia-oxidizing bacteria respond more strongly to nitrogen addition than ammonia-oxidizing archaea, Soil Biol. Biochem., 99, 158–166, doi:10.1016/j.soilbio.2016.05.014, 2016.

Castellano-Hinojosa, A., Correa-Galeote, D., Carrillo, P., Bedmar, E. J. and Medina-Sánchez, J. M.: Denitrification and biodiversity of denitrifiers in a High-Mountain Mediterranean Lake, Front.

560   Microbiol., 8, 1911, doi:10.3389/fmicb.2017.01911, 2017.

Chen, C. A., Wang, S., Lu, X., Zhang, S., Lui, H., Tseng, H., Wang, B. and Huang, H.: Hydrogeochemistry and greenhouse gases of the Pearl River, its estuary and beyond, Quaternary International, 186, 79–90, doi:10.1016/j.quaint.2007.08.024, 2008.

Chen, C. T. A.: Chemical and physical fronts in the Bohai, Yellow and East China seas, J. Mar. Syst.,

565   78(3), 394–410, doi:10.1016/j.jmarsys.2008.11.016, 2009.

Codispoti, L. A. and Christensen, J. P.: Nitrification, denitrification and nitrous oxide cycling in the eastern tropical South Pacific ocean, Mar. Chem., 16(4), 277–300, doi:http://dx.doi.org/10.1016/0304-4203(85)90051-9, 1985.

Cole, J. J. and Caraco, N. F.: Emissions of nitrous oxide (N_2O) from a tidal, freshwater river, the Hudson

570   River, New York, Environ. Sci. Technol., 35(6), 991–996, doi:10.1021/es0015848, 2001.

Conthe, M., Wittorf, L., Kuenen, J. G., Kleerebezem, R., Van Loosdrecht, M. C. M. and Hallin, S.: Life on N_2O: Deciphering the ecophysiology of N_2O respiring bacterial communities in a continuous culture, ISME J., 12(4), 1142–1153, doi:10.1038/s41396-018-0063-7, 2018.

Cui, P., Chen, Z., Zhao, Q., Yu, Z., Yi, Z., Liao, H. and Zhou, S.: Hyperthermophilic composting

575   significantly decreases N_2O emissions by regulating N_2O-related functional genes, Bioresour. Technol., 272(1), 433–441, doi:10.1016/j.biortech.2018.10.044, 2019.

Dai, M., Wang, L., Guo, X., Zhai, W., Li, Q., He, B. and Kao, S. J.: Nitrification and inorganic nitrogen distribution in a large perturbed river/estuarine system: The Pearl River Estuary, China, Biogeosciences, 5(5), 1227–1244, doi:10.5194/bg-5-1227-2008, 2008.

Biogeosciences
Discussions

580   Dai, M., Gan, J., Han, A., Kung, H. S. and Yin, Z.: Physical dynamics and biogeochemistry of the Pearl River plume, Biogeochem. Dyn. Major River-Coastal Interfaces, 321–352, doi:10.1017/cbo9781139136853.017, 2013.

Dang, H., Li, J., Chen, R., Wang, L., Guo, L., Zhang, Z. and Klotz, M. G.: Diversity, abundance, and spatial distribution of sedimet ammonia-oxidizing Betaproteobacteria in response to environmental

585   gradients and coastal eutrophication in Jiaozhou Bay, China, Appl. Environ. Microbiol., 76(14), 4691–4702, doi:10.1128/AEM.02563-09, 2010.

Domeignoz-Horta1, L. A., , AyméSpor 1, D. B., Breuil1, M.-C. and , Florian Bizouard1, J. L. and L. P.: The diversity of the N_2O reducers matters for the $N_2O:N_2$ denitrification end-product ratio across an annual and a perennial cropping system, Front. Microbiol, 6:971, doi:10.3389/fmicb.2015.00971, 2015.

590   Edgar, R.C: Search and clustering orders of magnitude faster than BLAST, Bioinformatics, 26, 2460–2461, doi:10.1093/bioinformatics/btq, 2010.

Fayazbakhsh, K., Abedian, A., Manshadi, B. D. and Khabbaz, R. S.: Introducing a novel method for materials selection in mechanical design using Z-transformation in statistics for normalization of material properties, Mater. Des., 30(10), 4396–4404, doi:10.1016/j.matdes.2009.04.004, 2009.

595   Francis, C. A., Roberts, K. J., Beman, J. M., Santoro, A. E. and Oakley, B. B.: Ubiquity and diversity of ammonia-oxidizing archaea in water columns and sediments of the ocean, Proc. Natl. Acad. Sci. U. S. A., 102(41), 14683–14688, doi:10.1073/pnas.0506625102, 2005.

Frey, C., Bange, H. W., Achterberg, E. P., Jayakumar, A. and Carolin, R.: Regulation of nitrous oxide production in low oxygen waters off the coast of Peru, Biogeosciences, doi:10.5194/bg-17-2263-2020,

600   2020.

Garnier, J., Cébron, A., Tallec, G., Billen, G., Sebilo, M. and Martinez, A.: Nitrogen behaviour and nitrous oxide emission in the tidal Seine River estuary (France) as influenced by human activities in the upstream watershed, Biogeochemistry, 77(3), 305–326, doi:10.1007/s10533-005-0544-4, 2006.

Hallin, S., Philippot, L., Löf, F. E., Sanford, R. A. and Jones, C. M.: Genomics and ecology of novel

605   N_2O-Reducing microorganisms, Trends Microbiol., 26, 43–55, doi:10.1016/j.tim.2017.07.003, 2018.

He, B., Dai, M., Zhai, W., Guo, X. and Wang, L.: Hypoxia in the upper reaches of the Pearl River Estuary and its maintenance mechanisms: A synthesis based on multiple year observations during 2000-2008, Mar. Chem., 167(July), 13–24, doi:10.1016/j.marchem.2014.07.003, 2014.

Henry, S., Bru, D., Stres, B., Hallet, S., and Philippot, L.: Quantitative detection of the *nosZ* gene, encoding nitrous oxide reductase, and comparison of the abundances of 16S rRNA, *narG*, *nirK*, and *nosZ* genes in soils, Appl. Environ. Microbiol., 72(8), 5181–5189, doi:10.1128/AEM.00231-06, 2006.

Hou, L., Xie, X., Wan, X., Kao, S. J., Jiao, N., and Zhang, Y.: Niche differentiation of ammonia and nitrite oxidizers along a salinity gradient from the Pearl River estuary to the South China Sea, Biogeosciences, 15(16), 5169–5187, doi:10.5194/bg-15-5169-2018, 2018.

Ji, Q., Buitenhuis, E., Suntharalingam, P., Sarmiento, J. L. and Ward, B. B.: Global nitrous oxide production determined by oxygen sensitivity of nitrification and denitrification, Global Biogeochem. Cycles, 32(12), 1790–1802, doi:10.1029/2018GB005887, 2018a.

Ji, Q., Frey, C., Sun, X., Jackson, M., Lee, Y., Jayakumar, A., Jeffrey, C. and Ward, B. B.: Nitrogen and oxygen availabilities control water column nitrous oxide production during seasonal anoxia in the Chesapeake Bay, Biogeosciences, 15, 6127–6138, doi:10.5194/bg-15-6127-2018, 2018b.

Jones, C. M., Graf, D. R. H., Bru, D., Philippot, L., and Hallin, S.: The unaccounted yet abundant nitrous oxide-reducing microbial community: a potential nitrous oxide sink, ISME J. 7, 417–26, doi:10.1038/ismej.2012.125, 2013.

Jones, C. M., Spor, A., Brennan, F. P., Breuil, M., Bru, D., Lemanceau, P., et al.: Recently identified microbial guild mediates soil N_2O sink capacity, Nat. Climate change. 4, 801–805, doi:10.1038/nclimate2301, 2014.

Jones, C. M., Stres, B., Rosenquist, M., and Hallin, S.: Phylogenetic analysis of nitrite, nitric oxide, and nitrous oxide respiratory enzymes reveal a complex evolutionary history for denitrification, Mol. Biol. Evol. 25, 1955–1966, doi:10.1093/molbev/msn146, 2008.

Katoh, K. and Standley, D. M.: MAFFT multiple sequence alignment software version 7: Improvements in performance and usability, Mol. Biol. Evol., 30(4), 772–780, doi:10.1093/molbev/mst010, 2013.

Kester, R. A., De Boer, W., and Laanbroek, H. J.: Production of NO and N_2O by pure cultures of nitrifying and denitrifying bacteria during changes in aeration, Appl. Environ. Microbiol., 63, 3872–3877, doi:10.1128/AEM.63.10.3872–3877, 1997.

635   Lam, P., Jensen, M. M., Lavik, G., McGinnis, D. F., Müller, B., Schubert, C. J., Amann, R., Thamdrup, B. and Kuypers, M. M. M.: Linking crenarchaeal and bacterial nitrification to anammox in the Black Sea, Proc. Natl. Acad. Sci. U. S. A., 104(17), 7104–7109, doi:10.1073/pnas.0611081104, 2007.

Laperriere, S. M., Nidzieko, N. J., Fox, R. J., Fisher, A. W. and Santoro, A. E.: Observations of variable ammonia oxidation and nitrous oxide flux in a eutrophic estuary, Estuaries and Coasts, 42(1), 33–44,
640   doi:10.1007/s12237-018-0441-4, 2019.

Lee, J. A., and Francis, C. A.: Spatiotemporal characterization of San Francisco Bay denitrifying communities: a comparison of *nirK* and *nirS* diversity and abundance. Microb. Ecol., 73(2), 271–284, doi:10.1007/s00248-016-0865-y, 2017.

Li, J., Nedwell, D. B., Beddow, J., Dumbrell, A. J., McKew, B. A., Thorpe, E. L. and Whitby, C.: *amoA*
645   gene abundances and nitrification potential rates suggest that benthic ammonia-oxidizing bacteria and not archaea dominate N cycling in the Colne estuary, United Kingdom, Appl. Environ. Microbiol., 81(1), 159–165, doi:10.1128/AEM.02654-14, 2015.

Li, Z., Jin, W., Liang, Z., Yue, Y. and Lv, J.: Abundance and diversity of ammonia-oxidizing archaea in response to various habitats in Pearl River Delta of China, a subtropical maritime zone, J. Environ. Sci.
650   (China), 25(6), 1195–1205, doi:10.1016/S1001-0742(12)60178-8, 2013.

Lin, J., Chen, N., Wang, F., Huang, Z., Zhang, X., and Liu, L.: Urbanization increased river nitrogen export to western Taiwan Strait despite increased retention by nitrification and denitrification, Ecol. Indic., 109, 105756, doi:10.1016/j.ecolind.2019.105756, 2020.

Löscher, C. R., Kock, A., Könneke, M., Laroche, J., Bange, H. W., and Schmitz, R. A.: Production of
655   oceanic nitrous oxide by ammonia-oxidizing archaea, Biogeosciences, 9, 2419–2429, doi:10.5194/bg-9-2419-2012, 2012.

Lu, Y., Cheung, S., Chen, L., Kao, S., Xia, X., Gan, J., et al.: New insight to niche partitioning and ecological function of ammonia oxidizing archaea in subtropical estuarine ecosystem, Biogeosciences, 17, 6017–6032, doi:10.5194/bg-17-6017-2020, 2020.

660   Ma, L., Lin, H., Xie, X., Dai, M., and Zhang, Y.: Major role of ammonia-oxidizing bacteria in N_2O

production in the Pearl River estuary, Biogeosciences, 16, 4765–4781, doi:10.5194/bg-16-4765-2019,

2019.

Marchant, H. K., Ahmerkamp, S., Lavik, G., Tegetmeyer, H. E., Graf, J., Klatt, J. M., Holtappels, M.,

Walpersdorf, E. and Kuypers, M. M. M.: Denitrifying community in coastal sediments performs aerobic

665   and anaerobic respiration simultaneously, ISME J. 11, 1799–1812, doi:10.1038/ismej.2017.51, 2017.

Martens-Habbena, W., and Stahl, D. A.: Nitrogen metabolism and kinetics of ammonia-oxidizing

archaea, Methods Enzymol., 496, 465–487, doi:10.1016/B978-0-12-386489-5.00019-1, 2011.

Marzadri, A., Dee, M. M., Tonina, D., Bellin, A., and Tank, J. L.: Role of surface and subsurface

processes in scaling N_2O emissions along riverine networks, Proc. Natl. Acad. Sci. U. S. A., 114(17),

670   4330–4335, doi:10.1073/pnas.1617454114, 2017.

Massana, R., Murray, A. E., Preston, C. M., and DeLong, E. F.: Vertical distribution and phylogenetic

characterization of marine planktonic archaea in the Santa Barbara Channel, Appl. Environ. Microbiol.,

63(1), 50–56, doi:10.1128/aem.63.1.50-56.1997, 1997.

Meinhardt, K. A., Stopnisek, N., Pannu, M. W., Strand, S. E., Fransen, S. C., Casciotti, K. L. and Stahl,

675   D. A.: Ammonia-oxidizing bacteria are the primary N_2O producers in an ammonia-oxidizing archaea

dominated alkaline agricultural soil, Environ. Microbiol., 20(6), 2195–2206, doi:10.1111/1462-

2920.14246, 2018.

Mosier, A. C., and Francis, C. A.: Denitrifier abundance and activity across the San Francisco Bay

estuary, Environ. Microbiol Rep., 2, 667–676, doi:10.1111/j.1758-2229.2010.00156.x, 2010.

680   Nakai, R., Nishijima, M., Tazato, N., Handa, Y., Karray, F., Sayadi, S., Isoda, H. and Naganuma, T.:

Oligoflexus tunisiensis gen. nov., sp. nov., a Gram-negative, aerobic, filamentous bacterium of a novel

proteobacterial lineage, and description of *Oligoflexaceae* fam. nov., *Oligoflexales* ord. nov. and

Oligoflexia classis nov, Int. J. Syst. Evol. Microbiol, 64, 3353–3359, doi:10.1099/ijs.0.060798-0, 2014.

Nevison, C., Butler, J. H., and Elkins, J. W.: Global distribution of N_2O and the ΔN_2O-AOU yield in the

685   subsurface ocean, Global Biogeochem. Cycles, 17, 1–18, doi:10.1029/2003GB002068, 2003.

Palacin-Lizarbe, C., Camarero, L., Hallin, S., Jones, C., Caliz, J., Casamayor, E. O. and Catalan, J.: The DNRA-denitrification dichotomy differentiates nitrogen transformation pathways in mountain lake benthic habitats, Front. Microbiol., 10, 1229, doi:10.3389/FMICB.2019.01229, 2019.

Philippot, L.: Loss in microbial diversity affects nitrogen cycling in soil, ISME J., 11, 1609–1619, 2013.

690 Price, M. N., Dehal, P. S., and Arkin, A. P.: FastTree 2 - Approximately maximum-likelihood trees for large alignments, PLoS One 5, 9490, doi:10.1371/journal.pone.0009490, 2010.

Xu Jirong, Wang Youshao, Wang Qinji, Yin Jianping: Nitrous oxide concentration and nitrification and denitrification in Zhujiang River Estuary, China. J. Environ. Sci., 18, 4. 122–130, doi:, 2005.

Qu, Z., Bakken, L. R., Molstad, L., Frostegård, Å., and Bergaust, L. L.: Transcriptional and metabolic
695 regulation of denitrification in Paracoccus denitrificans allows low but significant activity of nitrous oxide reductase under oxic conditions, Environ. Microbiol., 18, 2951–2963, doi:10.1111/1462-2920.13128, 2016.

Ravishankara, A. R., Daniel, J. S. and Portmann, R. W.: Nitrous oxide (N_2O): The dominant ozone-depleting substance emitted in the 21st century, Science, 326(5949), 123–125,
700 doi:10.1126/science.1176985, 2009.

Rissanen, A. J., Tiirola, M. and Ojala, A.: Spatial and temporal variation in denitrification and in the denitrifier community in a boreal lake, Aquat. Microb. Ecol., 64(1), 27–40, doi:10.3354/ame01506, 2011.

Riya, S., Takeuchi, Y., Zhou, S., Terada, A. and Hosomi, M.: Nitrous oxide production and mRNA expression analysis of nitrifying and denitrifying bacterial genes under floodwater disappearance and
705 fertilizer application, Environ. Sci. Pollut. Res., 24(18), 15852–15859, doi:10.1007/s11356-017-9231-y, 2017.

Rowley, G., Sullivan, M. J., Appia-Ayme, C., Gates, A. J. and Richardson, D. J.: Copper control of bacterial nitrous oxide emission and its impact on vitamin B12-dependent metabolism, Proc. Natl. Acad. Sci., 110(49), 19926–19931, doi:10.1073/pnas.1314529110, 2013.

710 Sanford, R. A., Wagner, D. D., Wu, Q. Z., Chee-Sanford, J. C., Thomas, S. H., Cruz-Garcia, C., Rodriguez, G., Massol-Deya, A., Krishnani, K. K., Ritalahti, K. M., Nissen, S., Konstantinidis, K. T. and Loffler, F. E.: Unexpected nondenitrifier nitrous oxide reductase gene diversity and abundance in soils, Proc. Natl. Acad. Sci. U. S. A., 109(48), 19709–19714, doi:10.1073/Pnas.1211238109, 2012.

715 Santoro, A. E., Buchwald, C., McIlvin, M. R., and Casciotti, K. L.: Isotopic Signature of N_2O Produced by Marine Ammonia-Oxidizing Archaea, Science, 333, 1282–1285, doi:10.1126/science.1208239, 2011.

Senbayram, M., Budai, A., Bol, R., Chadwick, D., Marton, L., Gündogan, R. and Wu, D.: Soil NO_3^- level and O_2 availability are key factors in controlling N_2O reduction to N_2 following long-term liming of an acidic sandy soil, Soil Biol. Biochem., 132(3), 165–173, doi:10.1016/j.soilbio.2019.02.009, 2019.

Shaw, L. J., Nicol, G. W., Smith, Z., Fear, J., Prosser, J. I., and Baggs, E. M.: *Nitrosospira spp.* can

720 produce nitrous oxide via a nitrifier denitrification pathway, Environ. Microbiol., 8, 214–222, doi:10.1111/j.1462-2920.2005.00882.x, 2006.

Shcherbak, I., Millar, N., and Robertson, G. P.: Global metaanalysis of the nonlinear response of soil nitrous oxide (N_2O) emissions to fertilizer nitrogen, Proc. Natl. Acad. Sci., 111, 9199–9204, doi:10.1073/pnas.1322434111, 2014.

725 Silvennoinen, H., Liikanen, A., Torssonen, J., Florian Stange, C., and Martikainen, P. J.: Denitrification and nitrous oxide effluxes in boreal, eutrophic river sediments under increasing nitrate load: A laboratory microcosm study, Biogeochemistry, 91(2–3), 105–116, doi:10.1007/s10533-008-9262-z, 2008.

Smith, C. J., Nedwell, D. B., Dong, L. F., and Osborn, A. M.: Diversity and abundance of nitrate reductase genes (*narG* and *napA*), nitrite reductase genes (*nirS* and *nrfA*), and their transcripts in estuarine

730 sediments, Appl. Environ. Microbiol., 73(11), 3612–3622, doi:10.1128/AEM.02894-06, 2007.

Song, D., Zhang, G., Li, P., and Liu, S.: Distribution and fluxes of nitrous oxide in the Bohai Sea in summer, Advances in Marine Sciences, 13–21, doi:10.12677/ams.2015.22003, 2015.

Song, K., Suenaga, T., Hamamoto, A., Satou, K., Riya, S., Hosomi, M. and Terada, A.: Abundance, transcription levels and phylogeny of bacteria capable of nitrous oxide reduction in a municipal

735 wastewater treatment plant, J. Biosci. Bioeng., 118(3), 289–297, doi:10.1016/j.jbiosc.2014.02.028, 2014.

Stieglmeier, M., Mooshammer, M., Kitzler, B., Wanek, W., Zechmeister-Boltenstern, S., Richter, A. and Schleper, C.: Aerobic nitrous oxide production through N-nitrosating hybrid formation in ammonia-oxidizing archaea, ISME J., 8(5), 1135–1146, doi:10.1038/ismej.2013.220, 2014.

Sun, X., Amal Jayakumar., John C. Tracey., Elizabeth Wallace., Colette L. Kelly., Karen L. Casciotti.,

740 Bess B. Ward.: Microbial N_2O consumption in and above marine N_2O production hotspots, ISME, 15, 1434–1444, doi:10.1038/s41396-020-00861-2, 2021.

Ter, C. J. F.: Canonical correspondence analysis: a new eigenvector technique for multivariate direct gradient analysis, Ecology, 67, 1167–1179, doi:10.2307/1938672, 1986.

Thompson, K.: Abundance, activity and community structure of nitrifier and denitrifier communities in

745   Agro-Ecosystems, A Thesis presented to The University of Guelph, 2016.

Wang, L., Zhang, G., Zhu, Z., Li, J., Liu, S., Ye, W. and Han, Y.: Distribution and sea-to-air flux of nitrous oxide in the East China Sea during the summer of 2013, Cont. Shelf Res., 123, 99–110, doi:10.1016/j.csr.2016.05.001, 2016.

Wang, L., Zheng, B., Nan, B., and Hu, P.: Diversity of bacterial community and detection of *nirS*- and

750   *nirK*-encoding denitrifying bacteria in sandy intertidal sediments along Laizhou Bay of Bohai Sea, China, Mar. Pollut. Bull., 88(1–2), 215–223, doi:10.1016/j.marpolbul.2014.09.002, 2014.

Wei, W., Isobe, K., Nishizawa, T., Zhu, L., Shiratori, Y., Ohte, N., Koba, K., Otsuka, S. and Senoo, K.: Higher diversity and abundance of denitrifying microorganisms in environments than considered previously, ISME J. 9(9), 1954–1965, doi:10.1038/ismej.2015.9, 2015.

755   De Wilde, H. P. J. and De Bie, M. J. M.: Nitrous oxide in the Schelde estuary: Production by nitrification and emission to the atmosphere, Mar. Chem., 69(3–4), 203–216, doi:10.1016/S0304-4203(99)00106-1, 2000.

Wittorf, L., Roger, F., Alsterberg, C., Gamfeldt, L., Hulth, S., Sundback, K., Jones, C. M. and Hallin, S.: Habitat diversity and type govern potential nitrogen loss by denitrification in coastal sediments and

760   differences in ecosystem-level diversities of disparate N_2O reducing communities, FEMS Microbiol. Ecol. 96(9), 1–9, doi:10.1093/femsec/fiaa091, 2020.

Wrage, N., Velthof, G. L., Van Beusichem, M. L., and Oenema, O.: Role of nitrifier denitrification in the production of nitrous oxide, Soil Biol. Biochem. 33(12–13), 1723–1732, doi:10.1016/S0038-0717(01)00096-7, 2001.

765   Wu, J., Chen, N., Hong, H., Lu, T., Wang, L., and Chen, Z.: Direct measurement of dissolved N_2 and denitrification along a subtropical river-estuary gradient, China. Mar. Pollut. Bull. 66(1–2), 125–134, doi:10.1016/j.marpolbul.2012.10.020, 2013.

Yamagishi, H., Westley, M. B., Popp, B. N., Toyoda, S., Yoshida, N., Watanabe, S., Koba, K. and Yamanaka, Y.: Role of nitrification and denitrification on the nitrous oxide cycle in the eastern tropical

770   North Pacific and Gulf of California, J. Geophys. Res., 112, 1–15, doi:10.1029/2006JG000227, 2007.

Yan, W., Yang, L., Wang, F., Wang, J., and Ma, P.: Riverine N_2O concentrations, exports to estuary and emissions to atmosphere from the Changjiang River in response to increasing nitrogen loads, Global Biogeochem. Cycles, 26(4), doi:10.1029/2010GB003984, 2012a.

Yan, X. L., Zhai, W. D., Hong, H. S., Li, Y., Guo, W. D., and Huang, X.: Distribution, fluxes and decadal

775   changes of nutrients in the Jiulong River Estuary, Southwest Taiwan Strait, Chinese Sci. Bull. 57(18), 2307–2318, doi:10.1007/s11434-012-5084-4, 2012b.

Yan, X., Wan, X. S., Liu, L., Xu, M. N., Tan, E., Zheng, Z., Zou, W., Tian, L., Li, D. W., Trull, T. W. and Kao, S. J.: Biogeochemical dynamics in a eutrophic tidal estuary revealed by isotopic compositions of multiple nitrogen species, Journal of Geophysical Research : Biogeosciences, 1849–1864,

780   doi:10.1029/2018JG004959, 2019.

Yan, X. L., Zhai, W. D., Hong, H. S., Li, Y., Guo, W. D. and Huang, X.: Distribution, fluxes and decadal changes of nutrients in the Jiulong River Estuary, Southwest Taiwan Strait, Chinese Sci. Bull., 57(18), 2307–2318, doi:10.1007/s11434-012-5084-4, 2012b.

Yao, Y., Tian, H., Shi, H., Pan, S., Xu, R., Pan, N., and Canadell, J. G.: Increased global nitrous oxide

785   emissions from streams and rivers in the Anthropocene, Nat. Clim. Chang., 10(2), 138–142, doi:10.1038/s41558-019-0665-8, 2020.

Yu, S., Yao, P., Liu, J., Zhao, B., Zhang, G., Zhao, M., Yu, Z. and Zhang, X. H.: Diversity, abundance, and niche differentiation of ammonia-oxidizing prokaryotes in mud deposits of the eastern China marginal seas, Front. Microbiol., 7(FEB), 1–13, doi:10.3389/fmicb.2016.00137, 2016.

790   Zhang, G. L., Zhang, J., Liu, S. M., Ren, J. L., and Zhao, Y. C.: Nitrous oxide in the Changjiang (Yangtze River) Estuary and its adjacent marine area: Riverine input, sediment release and atmospheric fluxes, Biogeosciences, 7(11), 3505–3516, doi:10.5194/bg-7-3505-2010, 2010.

Zhang, G., Zhang, J., Ren, J., Li, J., and Liu, S.: Distributions and sea-to-air fluxes of methane and nitrous oxide in the North East China Sea in summer, Mar. Chem., 110(1–2), 42–55,

795   doi:10.1016/j.marchem.2008.02.005, 2008.

Zhang, J.: Biogeochemistry of Chinese estuarine and coastal waters: nutrients, trace metals and biomarkers, J. Mater. Cycles Waste Manag., 3(1-3), 65–76, doi:10.1007/s10113-001-0039-3, 2002.

Zhang, Y., Xie, X., Jiao, N., Hsiao, S. S. Y., and Kao, S. J.: Diversity and distribution of *amoA*-type nitrifying and *nirS*-type denitrifying microbial communities in the Yangtze River estuary, Biogeosciences, 11(8), 2131–2145, doi:10.5194/bg-11-2131-2014, 2014.

Zhao, S., Wang, Q., Zhou, J., Yuan, D., and Zhu, G.: Linking abundance and community of microbial N_2O-producers and N_2O-reducers with enzymatic N_2O production potential in a riparian zone, Sci. Total Environ., 642, 1090–1099, doi:10.1016/J.SCITOTENV.2018.06.110, 2018.

Zheng, Z. Z., Wan, X., Xu, M. N., Hsiao, S. S. Y., Zhang, Y., Zheng, L. W., Wu, Y., Zou, W. and Kao, S. J.: Effects of temperature and particles on nitrification in a eutrophic coastal bay in southern China, J. Geophys. Res. Biogeosciences, 122(9), 2325–2337, doi:10.1002/2017JG003871, 2017.

Zhu, Z. Y., Zhang, J., Wu, Y., Zhang, Y. Y., Lin, J., and Liu, S. M.: Hypoxia off the Changjiang (Yangtze River) Estuary: Oxygen depletion and organic matter decomposition, Mar. Chem., 125(1–4), 108–116, doi:10.1016/j.marchem.2011.03.005, 2011.
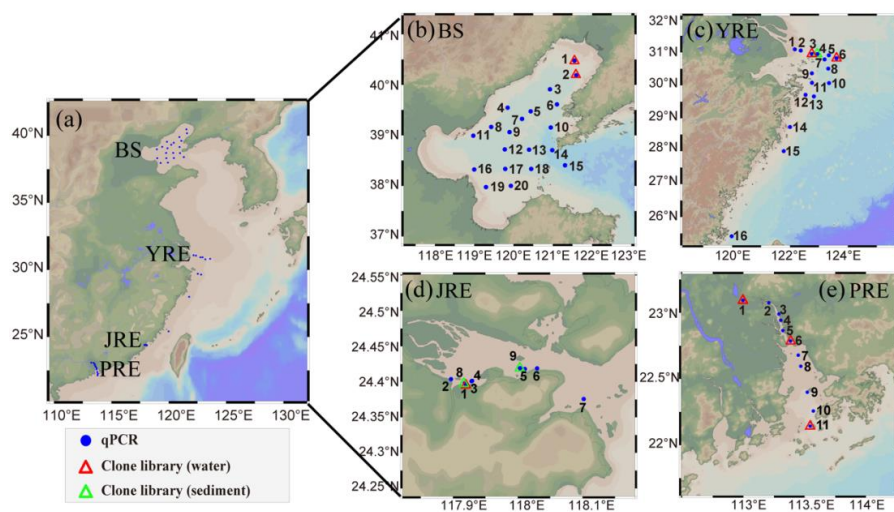
800

805

810

Figure 1. **(a)** Sampling sites in the four estuaries along China's coastline; **(b)** Bohai Sea (BS); **(c)** Yangtze River Estuary (YRE); **(d)** Jiulong River Estuary (JRE); **(e)** Pearl River Estuary (PRE). The figure was produced by Ocean Data View 5.2.0 (http://odv.awi.de/).
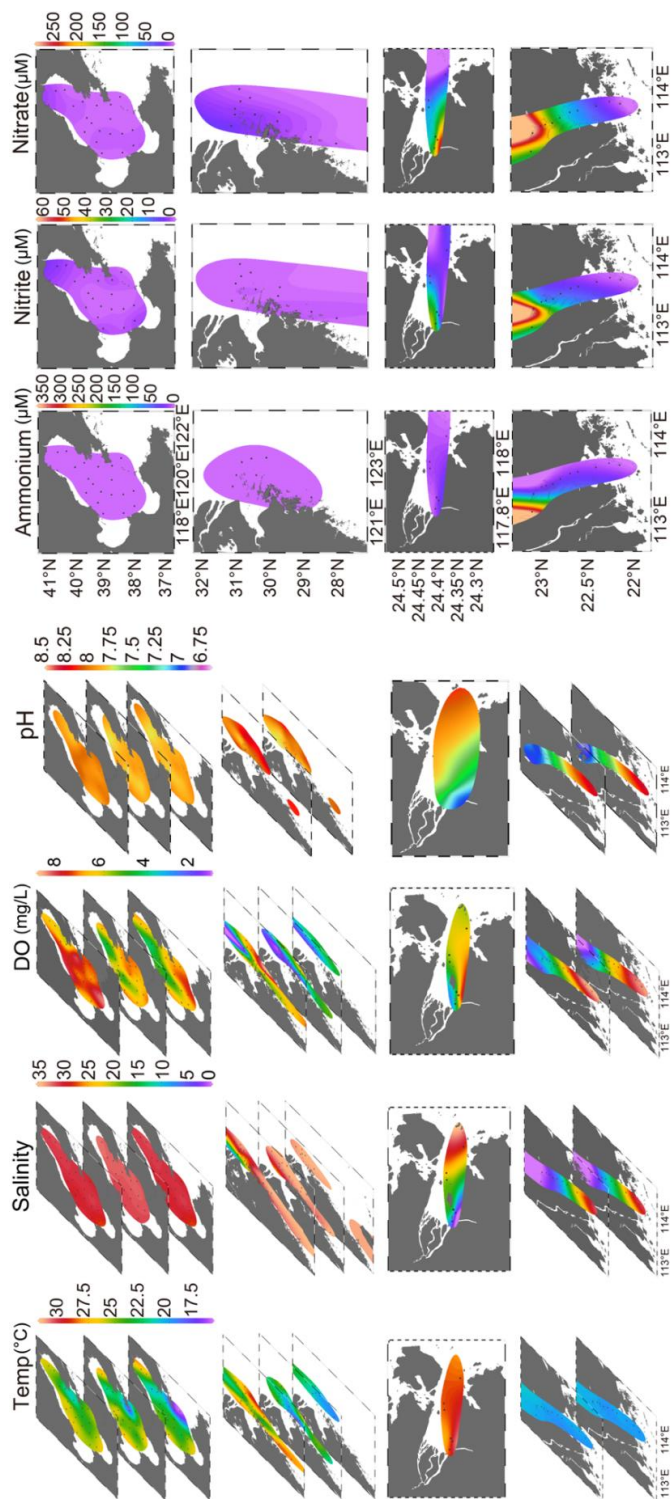
815

Figure 2. Temperature (Temp), salinity, dissolved oxygen (DO), pH, ammonium, nitrite, and nitrate concentration distributions in the four estuaries. Depth integrated mean values were used for ammonium, nitrite, and nitrate concentration distributions.
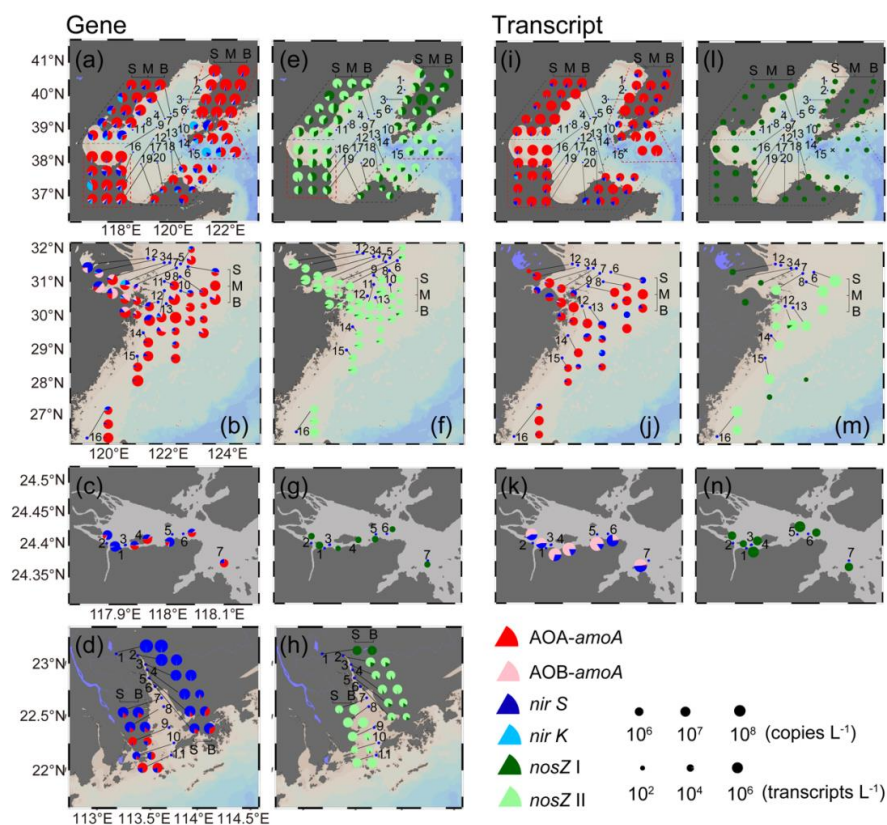
Figure 3. Six key functional gene and transcript abundance distributions in the four estuaries. S, surface layer; M, middle layer; B, bottom layer. **(a)**–**(d)** Gene related to N₂O production; **(e)**–**(h)** Gene related to N₂O consumption; **(i)**–**(k)** Transcript related to N₂O production; **(l)**–**(n)** Transcript related to N₂O consumption. **(a)**, **(e)**, **(i)**, and **(l)** Bohai Sea; **(b)**, **(f)**, **(j)**, and **(m)** Yangtze River Estuary; **(c)**, **(g)**, **(k)**, and **(n)** Jiulong River Estuary; **(d)** and **(h)** Pearl River Estuary.
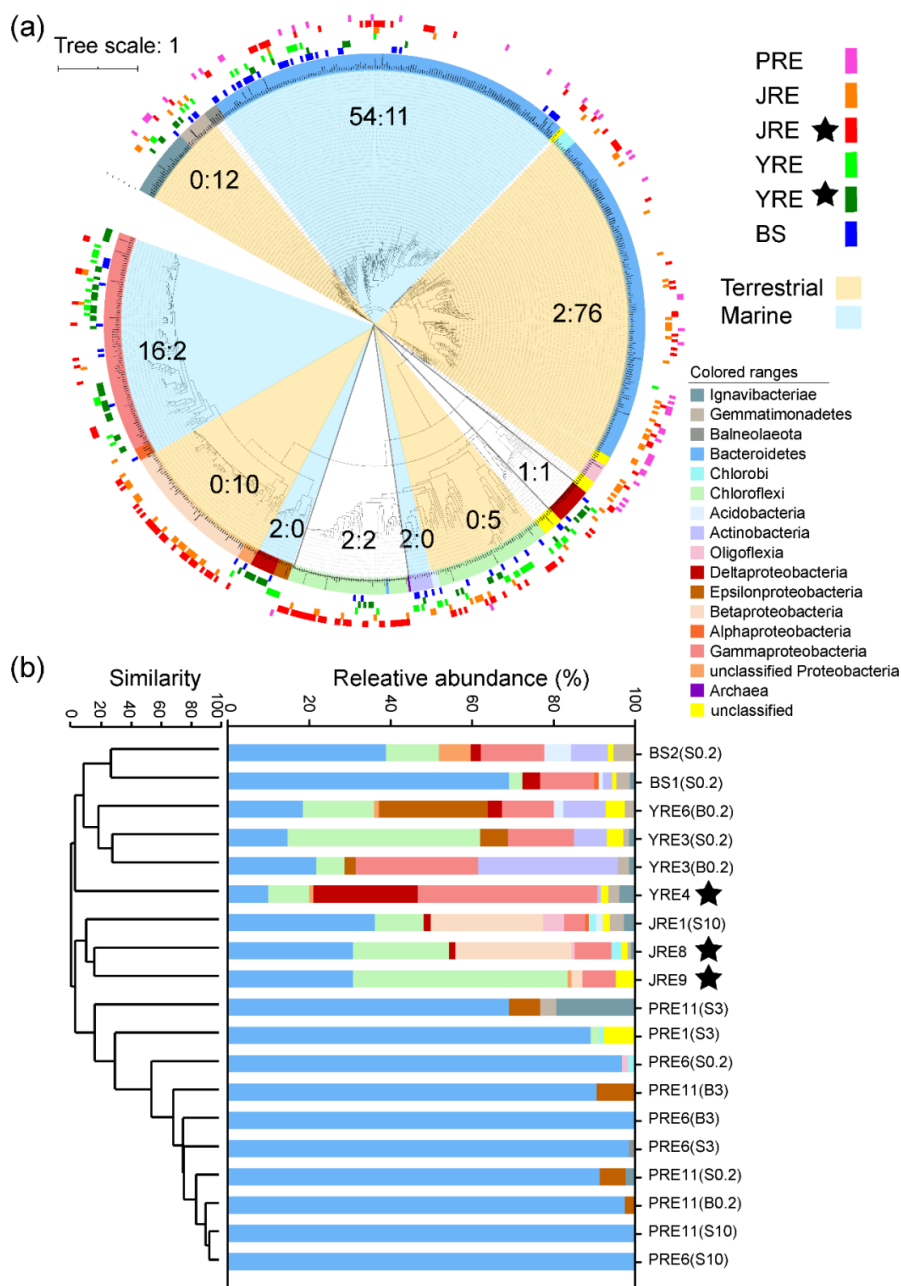
Figure 4. (a) Maximum likelihood phylogenetic tree of amino acid sequences of the clade II-type *nosZ*. The colors of the inner circle indicate taxonomic affiliations based on reference sequences. The colors of the outer circles represent the sources of clone sequences. The phylogenetic tree was bootstrapped 500 times. The scale bar represents the number of amino acid substitutions per site. Numbers before and after the colons indicate the number of reference sequences from marine and terrestrial habitats, respectively. The figure was produced using the interactive tree of

life (http://itol.embl.de/; Letunic and Bork 2016). **(b)** Relative abundances of community compositions of the clade

II-type *nosZ* gene clone libraries in the four estuaries. The colors of the bars indicate taxonomic affiliations. The

830 similarity was calculated from Bray–Curtis similarity. Black stars indicate sediment samples.
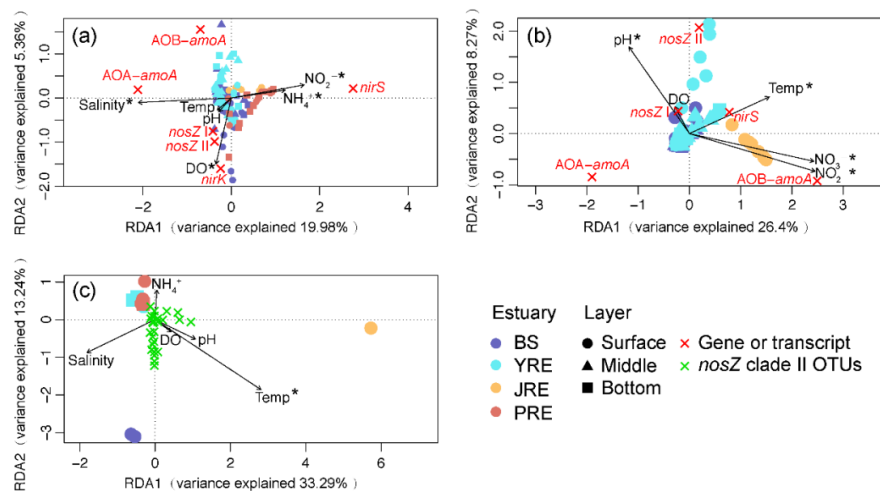
Figure 5. Redundancy analysis of the relative abundances of ammonia-oxidizing archaeal *amoA* (AOA-*amoA*), bacterial *amoA* (AOB-*amoA*), *nirS*, *nirK*, and *nosZ* clade I and II **(a)** genes and **(b)** transcripts, as well as of **(c)** the community composition of the *nosZ* clade II clone libraries under biogeochemical constraints. Each circle, triangle, or square represents an individual sample from the surface, middle, or bottom layer, respectively. The fork-shaped symbol represents the functional gene, transcript, or *nosZ* clade II OTU. Vectors represent environmental variables. Asterisks indicate statistically significant variables. Temp, temperature; DO, dissolved oxygen.
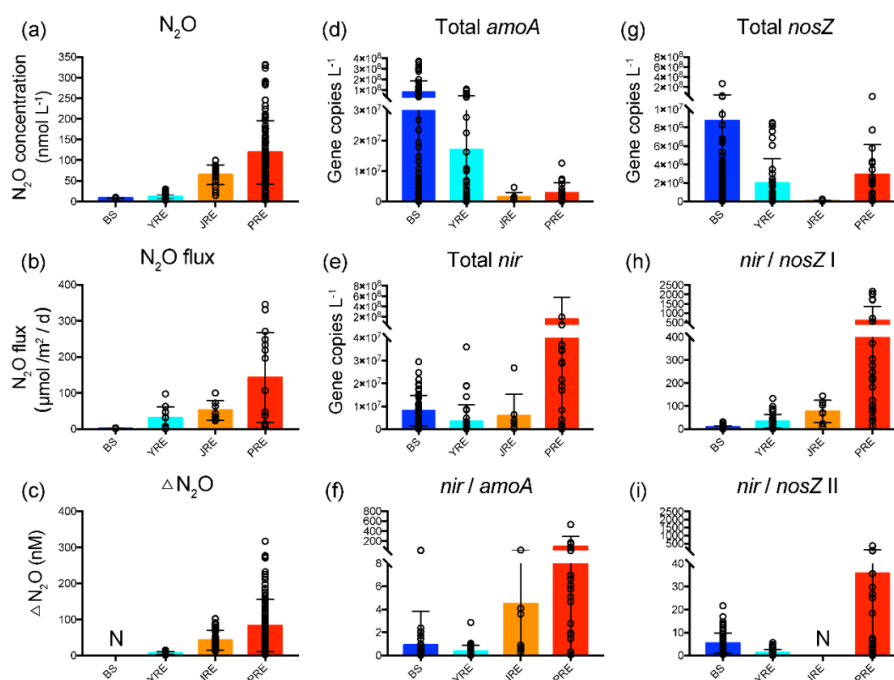
Figure 6. The ranges of **(a)** N_2O concentration, **(b)** N_2O flux, **(c)** ΔN_2O (data from Qinji, 2005; Chen et al., 2008; Zhang et al., 2008; Wu et al., 2013; Song et al., 2015; Wang et al., 2016; Ma et al., 2019; Lin et al., 2020), **(d)** total archaeal and bacterial *amoA* gene abundance, **(e)** total *nirS* and *nirK* gene abundance, **(f)** the ratio of total *nir* to *amoA* gene abundance, **(g)** total *nosZ* clade I and II gene abundance, **(h)** the ratio of total *nir* to *nosZ* clade I gene abundance, and **(i)** ratio of total *nir* to *nosZ* clade II gene abundance in the Bohai Sea (BS), Yangtze River estuary (YRE), Jiulong River estuary (JRE), and Pearl River estuary (PRE). Black circles represent the value of each sample. Bars represent the mean values. Error bars indicate standard deviation. N, no data or not determined.